Hotspot of Glyoxal Over the Pearl River Delta Seen from the OMI Satellite Instrument: Implications for Emissions of Aromatic Hydrocarbons

Christopher Chan Miller[1], Daniel J. Jacob[1,2], Gonzalo González Abad[3], and Kelly Chance[3]

[1]Department of Earth and Planetary Science, Harvard University, Cambridge MA, USA
[2]School of Engineering and Applied Sciences, Harvard University, Cambridge MA, USA
[3]Harvard-Smithsonian Center for Astrophysics, Cambridge MA, USA

Correspondence to: C. Chan Miller (cmiller@fas.harvard.edu)

Abstract. The Pearl River Delta (PRD) is a densely populated hub of industrial activity located in southern China. OMI satellite observations reveal a large hotspot of glyoxal (CHOCHO) over the PRD that is almost twice as large as any other in Asia. Formaldehyde (HCHO) and NO_2 observed by OMI are also high in the PRD but no more than in other urban/industrial areas of China. The CHOCHO hotspot over the PRD can be explained by industrial paint and solvent emissions of aromatic volatile organic compounds (VOCs), with toluene being a dominant contributor. By contrast, HCHO in the PRD originates mostly from VOCs emitted by combustion (principally vehicles). By applying a plume transport model to wind-segregated OMI data, we show that the CHOCHO and HCHO enhancements over the PRD observed by OMI are consistent with current VOC emission inventories. Prior work using CHOCHO retrievals from the SCIAMACHY satellite instrument suggested that emission inventories for aromatic VOCs in the PRD were too low by a factor of 10-20; we attribute this result in part to bias in the SCIAMACHY data and in part to underestimated CHOCHO yields from oxidation of aromatics. Our work points to the importance of better understanding CHOCHO yields from the oxidation of aromatics in order to interpret space-based CHOCHO observations in polluted environments.

1 Introduction

The Pearl River Delta (PRD) is a metropolis of nine cities on the southern coast of China with 57 million people as of 2013. Rapid economic growth over the past three decades has created a serious air quality problem within the region, with ozone (O_3) and particulate matter (PM) air quality standards frequently violated. Volatile organic compounds (VOCs) are important O_3 and PM precursors. Our recent retrieval of atmospheric glyoxal (CHOCHO) from the OMI satellite instrument, including a number of corrections to previous retrievals, finds the CHOCHO column concentrations over the PRD to be the highest in the world (Chan Miller et al., 2014). Here we use the OMI satellite data for CHOCHO and formaldehyde (HCHO) in the PRD to evaluate VOC emission inventories used by atmospheric models and the related VOC chemistry.

The PRD has undergone rapid industrialization since 1980 when a series of economic reforms reduced restrictions on foreign investment. The PRD is now referred to as the "World Factory", producing 25% of China's exports (Guangdong Statistical

Yearbook, 2010). Major industries include printing, oil refining, chemical production, automobile assembly, and electronics manufacturing (Zhong et al., 2013).

This industrialisation has led to worsening air quality throughout the region. Surface O_3 and PM are routinely in excess of Chinese national ambient air quality standards (Liu et al., 2013). Ozone production in the PRD is predominantly VOC-limited (Zhang et al., 2007, 2008; Wang et al., 2010; Shao et al., 2009; Xue et al., 2014), and the aromatic species toluene and xylene play a dominant role (Xue et al., 2014). Aromatics have also been identified as an important regional source of secondary organic aerosol via reactive uptake of their oxidation products (Li et al., 2013), including glyoxal (Fu et al., 2008).

CHOCHO is a high-yield product of aromatic oxidation (Nishino et al., 2010). Previous analyses of CHOCHO satellite observations over China have suggested that inventories of aromatic emissions are too low. Stavrakou et al. (2009) used 2005 observations of CHOCHO and HCHO from the SCIAMACHY satellite instrument and found the global RETRO VOC inventory (Maarten van het Bolscher, 2007) to be too low in the PRD by over a factor of 2. Liu et al. (2012) used 2007 SCIAMACHY CHOCHO observations and found the INTEX-B East Asian inventory (Zhang et al., 2009) to be too low in the PRD by a factor of 10 - 20.

Our OMI CHOCHO retrieval is systematically lower than the older SCIAMACHY data, with very different patterns, as a result of improved background corrections and removal of NO_2 interferences (Chan Miller et al., 2014). An independent OMI CHOCHO retrieval by Alvarado et al. (2014) is also systematically lower than SCIAMACHY. This calls for revisiting the interpretation of CHOCHO data from space. Focus on the PRD not only targets a hotspot in the OMI data, but enables comparison to a highly detailed local VOC inventory for the region (Zheng et al., 2009a, b).

2 Data and Methods

The Ozone Monitoring Instrument (OMI) was launched onboard the NASA Aura satellite in July 2004 (Levelt et al., 2006). Aura is in sun-synchronous orbit with an equatorial crossing time of 13:38 local. OMI measures backscattered solar radiation at a nadir spatial resolution of 13km$\times$24km and achieves daily global coverage by cross-track imaging. Spectral fitting yields slant columns of CHOCHO, HCHO and NO_2 along the optical path. These are converted to vertical columns using air mass factors (AMFs) that combine scattering weights and vertical concentration profiles (González Abad et al., 2015). We use CHOCHO data from Chan Miller et al. (2014), and HCHO and NO_2 data from the OMI Version 3 product release (González Abad et al., 2015; Bucsela et al., 2013). Vertical profiles for the AMF computation are from the GEOS-Chem chemical transport model (v9-01-3; http://geos-chem.org). GEOS-Chem was originally described by Bey et al. (2001) and the glyoxal simulation was first introduced by Fu et al. (2008). The chemical mechanism in v9-01-3 is described in Mao et al. (2013).

Observations are averaged on a $0.25^\circ \times 0.3125^\circ$ grid using an area-weighted tessellation algorithm (Spurr, 2004). We exclude observations from the first and last cross track positions, those that fail the retrieval algorithm statistical quality checks, and those impacted by the row anomaly (http://www.knmi.nl/omi/research/product/rowanomaly-background.php). Validation with aircraft data indicates that the OMI HCHO and NO_2 retrievals are accurate within 20% and 30% respectively (Lamsal et al.,

2014; Zhu et al., 2016). CHOCHO/HCHO column ratios from OMI are consistent with aircraft observations (Kaiser et al., 2015), whereas previous SCIAMACHY retrievals showed large discrepancies (DiGangi et al., 2012).

We relate the CHOCHO and HCHO satellite observations over the PRD to VOC emissions using a 1-D advective-reactive plume model (Beirle et al., 2011; Valin et al., 2013), assuming a constant wind u, and treating the PRD as a Gaussian-distributed source ($N(x;\sigma)$) orthogonal to the wind with total emission rate E_i (e.g. mol s^{-1}). Let l_i represent the vertical column density of VOC species i integrated in the horizontal orthogonally to the wind (molecules cm^{-1}). The continuity equation is written;

$$\frac{\partial l_i(x,t)}{\partial t} + u\frac{\partial l_i(x,t)}{\partial x} = E_i(t)N(x;\sigma) - k_i[OH](t)l_i(x,t) \quad (1)$$

Here k_i is the rate constant of the reaction of VOC i with the hydroxyl radical OH (the main sink for the VOCs of interest). The local diurnally-varying concentration of OH is calculated from GEOS-Chem and peaks at 1.5×10^7 molecules cm^{-3} at local noon, close to observed values in the PRD (Hofzumahaus et al., 2009). E_i varies diurnally using source scaling factors from GEOS-Chem (van Donkelaar et al., 2008). We use the NO_2 plume as a proxy to derive the along-trajectory width of the VOC source region (σ), using the exponential decay model from Beirle et al. (2011). The derived half-maximum width (~ 85 km) is reasonable given the observed extent of PRD urban landcover from MODIS.

CHOCHO is treated as a product of VOC oxidation with yield α_i from VOC i, and is lost by reaction with OH and photolysis (rate constants k_g and J_g respectively). The CHOCHO vertical column density integrated in the horizontal orthogonal to the wind ($g(x,t)$) is then given by

$$\frac{\partial g(x,t)}{\partial t} + u\frac{\partial g(x,t)}{\partial x} = \sum_i \alpha_i k_i[OH](t)l_i(x,t) - \{k_g[OH](t) + J_g(t)\}\, g(x,t) \quad (2)$$

A similar equation holds for HCHO. J_g is calculated using the Fast-JX radiative transfer model (Wild et al., 2000; Neu et al., 2007). The yields (α_i) are calculated for a 1-day VOC aging time using the box model simulation of Palmer et al. (2006) with the MCMv3.2 chemical mechanism(Jenkin et al., 1997, 2003; Bloss et al., 2005), and assuming a high-NO_x regime where organic peroxy radical products of VOC oxidation react mainly with NO.

We apply the plume model to VOC emissions from five different inventories - RETRO (Maarten van het Bolscher, 2007), MACCity (Granier et al., 2011), REASv2 (Kurokawa et al., 2013), INTEX-B (Zhang et al., 2009), and the local PRD inventory from Zheng et al. (2009a).

3 Results and Discussion

Figure 1 shows the mean 2006-2007 vertical columns of CHOCHO, HCHO, and tropospheric NO_2 over China. OMI CHOCHO columns in the PRD (23°N, 113°E) peak at 1.0×10^{15} molecules cm^2, the highest in the world on an annual basis (Chan Miller et al., 2014). HCHO in the PRD is also high but comparable to values in the industrial Szechuan Basin to the northwest and in the densely populated East China Plain. NO_2 is high but less than in the East China Plain. As pointed out previously by Liu

et al. (2012) and Li et al. (2014), the unusually high CHOCHO concentrations over the PRD can be attributed to high emissions of aromatic VOCs.

The Zheng et al. (2009a) PRD emissions inventory includes detailed VOC speciation profiles of local sources (Liu et al., 2008a; Lai et al., 2009), resolving 91 individual VOCs, and adds biogenic VOC emissions from GloBEIS (Zheng et al., 2009c). The inventory does not contain primary CHOCHO emissions, and primary HCHO emissions are negligibly small.

Figure 2 shows the VOC emissions from Zheng et al. (2009a) and the corresponding HCHO and CHOCHO production rates. Aromatic VOCs have higher CHOCHO yields than other precursors, and their emissions are high enough to dominate CHOCHO production. Paints and solvents are the largest source of aromatics in the inventory, responsible for over 50% of benzene, toluene and xylene emissions. Atmospheric VOC observations in the PRD are consistent with that solvent/paint signature (Liu et al., 2008b; Barletta et al., 2008), in contrast to other Chinese cities where VOC emissions are predominantly from combustion (Barletta et al., 2005). Acetylene emitted from combustion has a 64% ultimate yield of CHOCHO (Fu et al., 2008) but its lifetime is too long (about 10 days) to make a major contribution to the local CHOCHO budget.

HCHO is produced with a more consistent yield from different VOCs, as shown in Figure 2. VOCs emitted by vehicles including alkenes and $\geq C_4$ alkanes play a dominant role in HCHO production, with biogenic isoprene making an additional seasonal contribution. This explains why OMI HCHO columns in the PRD are comparable to other Chinese urban areas (Figure 1).

Figure 3 shows mean 2006-2007 OMI columns over the PRD segregated by northeasterly, easterly, and calm (< 2 m s^{-1}) wind conditions. The segregation is based on GEOS-5 surface wind data at Shenzhen (23.5°N, 114°E). The shape of the urban plume is consistent with wind direction. 90% of northeasterly conditions are in fall and winter. 50% of calm conditions are in summer, and easterly conditions are evenly spread over the seasons. These seasonal dependences explain the higher HCHO columns under calm conditions, as biogenic VOCs make a larger contribution in summer (Zheng et al., 2010). On the other hand, NO_2 is lower because of faster photochemical loss. CHOCHO shows much less variability between wind sectors, consistent with a dominant anthropogenic source and with photochemistry driving both production and loss.

We select observations from the northeasterly sector for application of the advective-reactive plume model to evaluate emission inventories. Wind under these conditions is relatively steady, with low diurnal variability, and the urban plume is transported over flat terrain. The prevailing fall/winter conditions minimize the influence of biogenic VOCs.

Figure 4 shows cross-wind integrals of CHOCHO and HCHO vertical column densities as a function of transport time calculated using the Zheng et al. (2009a) local inventory along the mean flow trajectories, and initialised upwind of the PRD. A regional background has been subtracted prior to integration using observations in a sector upwind of the plume source (114-116°E, 22-23°N). We ascribe a 20% relative error to the observations from systematic AMF uncertainties (Vrekoussis et al., 2010) and a spatially-uniform error from uncertainty in the background column value (Zhu et al., 2014).

Also shown in Figure 4 are the results from the advective-reactive plume model using the Zheng et al. (2009a) PRD emission inventory for individual VOCs, with MCMv3.2 yields for HCHO and CHOCHO (Figure 2). The model does not include biogenic emissions (isoprene, monoterpenes, and methanol), which are relatively weak in fall/winter and would be included in

the regional background. The anthropogenic emissions are released at $t = 6.5$ h for CHOCHO and $t = 7$ h for HCHO, based on the location of the observed maximum column of each species during calm conditions (Figure 3).

Figure 4 shows that the model can generally replicate the observed concentrations (line densities) of CHOCHO and HCHO as a function of transport time. We do not expect the model to perfectly replicate the shape of the plume, due to its simplistic treatment of transport, spatiotemporal allocation of emissions, and chemistry. Comparison of the integrated plume totals of the model and OMI is more robust. Specification of OH concentrations and photolysis rates is a source of uncertainty in the modeled plume total. We estimate a 30% uncertainty in OH concentrations, and a 20% uncertainty for photolysis rates, with the latter driven by aerosol scattering (Martin et al., 2003). Integrating the plume model results between $t = 5$ and $t = 20$ h in Figure 4, we find good agreement with OMI for both CHOCHO (370 ± 50 kmol modeled vs 350 ± 90 kmol OMI) and HCHO (3.2 ± 0.6 Mmol modeled vs 2.6 ± 0.7 Mmol OMI), and conclude that the PRD inventory of Zheng et al. (2009a) is consistent with observations.

We repeated the same plume model calculation with the INTEX-B, REASv2, RETRO, and MACCity emission inventories for the PRD. All inventories are for 2006 except RETRO (2000). Figure 5 shows the emissions from each inventory, together with integrated CHOCHO and HCHO plume enhancements in the PRD integrating the OMI observations and plume model results in Figure 4 between $t = 5$ and $t = 20$ h. With the exception of RETRO, all inventories have similar total VOC emissions on a per C basis, though they differ in speciation, and they reproduce the observed CHOCHO and HCHO plumes within 40% for CHOCHO and 55% for HCHO.

The good agreement between VOC emission inventories and satellite observations of CHOCHO and HCHO is in sharp disagreement with Liu et al. (2012), who inferred a 10 - 20-fold underestimation of PRD aromatic emissions in the INTEX-B inventory using SCIAMACHY CHOCHO observations. The same inventory in our plume model underestimates the OMI CHOCHO concentration by only a factor of 2. Increasing aromatic VOC emissions by a factor of 10 would also overestimate HCHO by more than a factor of 2.

Annually averaged SCIAMACHY CHOCHO columns are $\sim 60\%$ higher than OMI in the PRD, but this is not enough to explain the difference. Different aromatic CHOCHO yields likely play a larger role. Molar yields of CHOCHO in Liu et al. (2012) were 25% for benzene, 16% for toluene, and 16% for xylenes, based on a literature-based average of chamber experiments compiled by Fu et al. (2008). By contrast the MCMv3.2 molar yields used here are 75% for benzene, 70% for toluene, and 36% for xylenes.

Figure 6 shows the pathways to CHOCHO formation from toluene in MCMv3.2. Approximately half of CHOCHO formation in MCMv3.2 is produced as a first generation product via a bicyclic intermediate (TLBIPERO). The rest of CHOCHO production involves intermediate products, implying delays and additional uncertainties.

Studies reporting CHOCHO yields at the lower end of the range reported in Fu et al. (2008) were conducted under very high NO_x conditions, resulting in OH-adduct reactions (pink pathway, Figure 6) that would suppress CHOCHO formation (Nishino et al., 2010). The highest yield of $39.0 \pm 10.2\%$ measured by Volkamer et al. (2001) was performed under NO_x levels closer to ambient conditions, however it was later revised to $30.6 \pm 6.0\%$ after CHOCHO measurements from the experiment were revised downward based on more accurate CHOCHO absorption cross sections (Volkamer et al., 2005). Nishino et al. (2010)

corrected for NO_2 reactions in their kinetics analysis to determine a yield of $26.0 \pm 2.2\%$, in close agreement with Volkamer et al. (2001). In both studies, CHOCHO production was solely from first-generation production. This is very consistent with the 32% first-generation CHOCHO yield from MCMv3.2 via TLBIPERO (Figure 6). Thus the higher yield of CHOCHO from toluene in the MCMv3.2 mechanism relative to the Fu et al. (2008) compilation is due to the accounting of later-generation production.

Bloss et al. (2005) experimentally observed CHOCHO production from butenedial (MALDIAL), confirming the existence of later-generation CHOCHO production from toluene. Other later-generation CHOCHO formation pathways in MCMv3.2 still need to be experimentally confirmed. However, the combined data on CHOCHO and HCHO from the satellite observations do provide additional constraints. If the CHOCHO yield from aromatics were much lower than MCMv3.2, then aromatic emissions would need to be increased in a way that would be inconsistent with the HCHO data.

In conclusion, the CHOCHO hotspot over the Pearl River Delta seen by the OMI satellite instrument can be explained by a very large industrial source of aromatic VOCs, consistent with current emission inventories used in atmospheric models. There has been little confidence in the past in interpreting CHOCHO data from space, in part because of inconsistency with surface observations (DiGangi et al., 2012). This issue seems to be resolved with the OMI observations (Chan Miller et al., 2014), and we find CHOCHO to be an excellent tracer of aromatic VOC emissions where these are high. Further work will need to examine other sources of CHOCHO relevant to interpreting satellite observations, in particular biogenic isoprene. The multi-generation CHOCHO yields from the atmospheric oxidation of aromatic VOCs also needs to be better established.

Acknowledgements. This work was supported by the NASA Aura Science Team.

References

Alvarado, L. M. A., Richter, A., Vrekoussis, M., Wittrock, F., Hilboll, A., Schreier, S. F., and Burrows, J. P.: An improved glyoxal retrieval from OMI measurements, Atmospheric Measurement Techniques, 7, 4133–4150, doi:10.5194/amt-7-4133-2014, http://www.atmos-meas-tech.net/7/4133/2014/, 2014.

Barletta, B., Meinardi, S., Sherwood Rowland, F., Chan, C.-Y., Wang, X., Zou, S., Yin Chan, L., and Blake, D. R.: Volatile organic compounds in 43 Chinese cities, Atmospheric Environment, 39, 5979–5990, http://www.sciencedirect.com/science/article/pii/S1352231005005510, 2005.

Barletta, B., Meinardi, S., Simpson, I. J., Zou, S., Rowland, F. S., and Blake, D. R.: Ambient mixing ratios of nonmethane hydrocarbons (NMHCs) in two major urban centers of the Pearl River Delta (PRD) region: Guangzhou and Dongguan, Atmospheric Environment, 42, 4393 – 4408, doi:http://dx.doi.org/10.1016/j.atmosenv.2008.01.028, http://www.sciencedirect.com/science/article/pii/S1352231008000289, 2008.

Beirle, S., Boersma, K. F., Platt, U., Lawrence, M. G., and Wagner, T.: Megacity Emissions and Lifetimes of Nitrogen Oxides Probed from Space, Science, 333, 1737–1739, doi:10.1126/science.1207824, http://www.sciencemag.org/content/333/6050/1737.abstract, 2011.

Bey, I., Jacob, D. J., Yantosca, R. M., Logan, J. A., Field, B. D., Fiore, A. M., Li, Q., Liu, H. Y., Mickley, L. J., and Schultz, M. G.: Global modeling of tropospheric chemistry with assimilated meteorology: Model description and evaluation, Journal of Geophysical Research: Atmospheres, 106, 23 073–23 095, doi:10.1029/2001JD000807, http://dx.doi.org/10.1029/2001JD000807, 2001.

Bloss, C., Wagner, V., Jenkin, M. E., Volkamer, R., Bloss, W. J., Lee, J. D., Heard, D. E., Wirtz, K., Martin-Reviejo, M., Rea, G., Wenger, J. C., and Pilling, M. J.: Development of a detailed chemical mechanism (MCMv3.1) for the atmospheric oxidation of aromatic hydrocarbons, Atmospheric Chemistry and Physics, 5, 641–664, doi:10.5194/acp-5-641-2005, http://www.atmos-chem-phys.net/5/641/2005/, 2005.

Bucsela, E. J., Krotkov, N. A., Celarier, E. A., Lamsal, L. N., Swartz, W. H., Bhartia, P. K., Boersma, K. F., Veefkind, J. P., Gleason, J. F., and Pickering, K. E.: A new stratospheric and tropospheric NO_2 retrieval algorithm for nadir-viewing satellite instruments: applications to OMI, Atmospheric Measurement Techniques, 6, 2607–2626, doi:10.5194/amt-6-2607-2013, http://www.atmos-meas-tech.net/6/2607/2013/, 2013.

Chan Miller, C., Gonzalez Abad, G., Wang, H., Liu, X., Kurosu, T., Jacob, D. J., and Chance, K.: Glyoxal retrieval from the Ozone Monitoring Instrument, Atmospheric Measurement Techniques, 7, 3891–3907, doi:10.5194/amt-7-3891-2014, http://www.atmos-meas-tech.net/7/3891/2014/, 2014.

DiGangi, J. P., Henry, S. B., Kammrath, A., Boyle, E. S., Kaser, L., Schnitzhofer, R., Graus, M., Turnipseed, A., Park, J.-H., Weber, R. J., Hornbrook, R. S., Cantrell, C. A., Maudlin III, R. L., Kim, S., Nakashima, Y., Wolfe, G. M., Kajii, Y., Apel, E., Goldstein, A. H., Guenther, A., Karl, T., Hansel, A., and Keutsch, F. N.: Observations of glyoxal and formaldehyde as metrics for the anthropogenic impact on rural photochemistry, Atmospheric Chemistry and Physics, 12, 9529–9543, doi:10.5194/acp-12-9529-2012, http://www.atmos-chem-phys.net/12/9529/2012/, 2012.

Fu, T.-M., Jacob, D. J., Wittrock, F., Burrows, J. P., Vrekoussis, M., and Henze, D. K.: Global budgets of atmospheric glyoxal and methylglyoxal, and implications for formation of secondary organic aerosols, J. Geophys. Res., 113, http://dx.doi.org/10.1029/2007JD009505, 2008.

González Abad, G., Liu, X., Chance, K., Wang, H., Kurosu, T. P., and Suleiman, R.: Updated Smithsonian Astrophysical Observatory Ozone Monitoring Instrument (SAO OMI) formaldehyde retrieval, Atmospheric Measurement Techniques, 8, 19–32, doi:10.5194/amt-8-19-2015, http://www.atmos-meas-tech.net/8/19/2015/, 2015.

Granier, C., Bessagnet, B., Bond, T., D'Angiola, A., Denier van der Gon, H., Frost, G., Heil, A., Kaiser, J., Kinne, S., Klimont, Z., Kloster, S., Lamarque, J.-F., Liousse, C., Masui, T., Meleux, F., Mieville, A., Ohara, T., Raut, J.-C., Riahi, K., Schultz, M., Smith, S., Thompson, A., van Aardenne, J., van der Werf, G., and van Vuuren, D.: Evolution of anthropogenic and biomass burning emissions of air pollutants at global and regional scales during the 1980–2010 period, Climate Change, 109, 163–190, doi:10.1007/s10584-011-0154-1, http://dx.doi.org/10.1007/s10584-011-0154-1, 2011.

Hofzumahaus, A., Rohrer, F., Lu, K., Bohn, B., Brauers, T., Chang, C.-C., Fuchs, H., Holland, F., Kita, K., Kondo, Y., Li, X., Lou, S., Shao, M., Zeng, L., Wahner, A., and Zhang, Y.: Amplified Trace Gas Removal in the Troposphere, Science, 324, 1702–1704, doi:10.1126/science.1164566, http://www.sciencemag.org/content/324/5935/1702.abstract, 2009.

Jenkin, M. E., Saunders, S. M., and Pilling, M. J.: The tropospheric degradation of volatile organic compounds: a protocol for mechanism development, Atmospheric Environment, 31, 81 – 104, doi:http://dx.doi.org/10.1016/S1352-2310(96)00105-7, http://www.sciencedirect.com/science/article/pii/S1352231096001057, 1997.

Jenkin, M. E., Saunders, S. M., Wagner, V., and Pilling, M. J.: Protocol for the development of the Master Chemical Mechanism, MCM v3 (Part B): tropospheric degradation of aromatic volatile organic compounds, Atmospheric Chemistry and Physics, 3, 181–193, doi:10.5194/acp-3-181-2003, http://www.atmos-chem-phys.net/3/181/2003/, 2003.

Kaiser, J., Wolfe, G. M., Min, K. E., Brown, S. S., Miller, C. C., Jacob, D. J., deGouw, J. A., Graus, M., Hanisco, T. F., Holloway, J., Peischl, J., Pollack, I. B., Ryerson, T. B., Warneke, C., Washenfelder, R. A., and Keutsch, F. N.: Reassessing the ratio of glyoxal to formaldehyde as an indicator of hydrocarbon precursor speciation, Atmospheric Chemistry and Physics, 15, 7571–7583, doi:10.5194/acp-15-7571-2015, http://www.atmos-chem-phys.net/15/7571/2015/, 2015.

Kurokawa, J., Ohara, T., Morikawa, T., Hanayama, S., Janssens-Maenhout, G., Fukui, T., Kawashima, K., and Akimoto, H.: Emissions of air pollutants and greenhouse gases over Asian regions during 2000–2008: Regional Emission inventory in ASia (REAS) version 2, Atmospheric Chemistry and Physics, 13, 11 019–11 058, doi:10.5194/acp-13-11019-2013, http://www.atmos-chem-phys.net/13/11019/2013/, 2013.

Lai, C.-H., Chang, C.-C., Wang, C.-H., Shao, M., Zhang, Y., and Wang, J.-L.: Emissions of liquefied petroleum gas (LPG) from motor vehicles, Atmospheric Environment, 43, 1456 – 1463, doi:http://dx.doi.org/10.1016/j.atmosenv.2008.11.045, http://www.sciencedirect.com/science/article/pii/S1352231008010996, natural and Biogenic Emissions of Environmentally Relevant Atmospheric Trace Constituents in Europe, 2009.

Lamsal, L. N., Krotkov, N. A., Celarier, E. A., Swartz, W. H., Pickering, K. E., Bucsela, E. J., Gleason, J. F., Martin, R. V., Philip, S., Irie, H., Cede, A., Herman, J., Weinheimer, A., Szykman, J. J., and Knepp, T. N.: Evaluation of OMI operational standard NO2 column retrievals using in situ and surface-based NO_2 observations, Atmospheric Chemistry and Physics, 14, 11 587–11 609, 2014.

Levelt, P., van den Oord, G., Dobber, M., Malkki, A., Visser, H., de Vries, J., Stammes, P., Lundell, J., and Saari, H.: The ozone monitoring instrument, Geoscience and Remote Sensing, IEEE Transactions on, 44, 1093–1101, doi:10.1109/TGRS.2006.872333, 2006.

Li, N., Fu, T.-M., Cao, J., Lee, S., Huang, X.-F., He, L.-Y., Ho, K.-F., Fu, J. S., and Lam, Y.-F.: Sources of secondary organic aerosols in the Pearl River Delta region in fall: Contributions from the aqueous reactive uptake of dicarbonyls, Atmospheric Environment, 76, 200 – 207, doi:http://dx.doi.org/10.1016/j.atmosenv.2012.12.005, http://www.sciencedirect.com/science/article/pii/S1352231012011545, improving Regional Air Quality over the Pearl River Delta and Hong Kong: from Science to Policy, 2013.

Li, X., Rohrer, F., Brauers, T., Hofzumahaus, A., Lu, K., Shao, M., Zhang, Y. H., and Wahner, A.: Modeling of HCHO and CHOCHO at a semi-rural site in southern China during the PRIDE-PRD2006 campaign, Atmospheric Chemistry and Physics, 14, 12 291–12 305, doi:10.5194/acp-14-12291-2014, http://www.atmos-chem-phys.net/14/12291/2014/, 2014.

Liu, H., Wang, X. M., Pang, J. M., and He, K. B.: Feasibility and difficulties of China's new air quality standard compliance: PRD case of $PM_{2.5}$ and ozone from 2010 to 2025, Atmospheric Chemistry and Physics, 13, 12 013–12 027, doi:10.5194/acp-13-12013-2013, http://www.atmos-chem-phys.net/13/12013/2013/, 2013.

Liu, Y., Shao, M., Fu, L., Lu, S., Zeng, L., and Tang, D.: Source profiles of volatile organic compounds (VOCs) measured in China: Part I, Atmospheric Environment, 42, 6247 – 6260, doi:http://dx.doi.org/10.1016/j.atmosenv.2008.01.070, http://www.sciencedirect.com/science/article/pii/S1352231008000721, pRIDE-PRD 2004 Campaign : Program of Regional Integrated Experiments on Air Quality over Pearl River Delta of China, 2008a.

Liu, Y., Shao, M., Lu, S., Chang, C.-C., Wang, J.-L., and Fu, L.: Source apportionment of ambient volatile organic compounds in the Pearl River Delta, China: Part {II}, Atmospheric Environment, 42, 6261 – 6274, doi:http://dx.doi.org/10.1016/j.atmosenv.2008.02.027, http://www.sciencedirect.com/science/article/pii/S1352231008001647, pRIDE-PRD 2004 Campaign : Program of Regional Integrated Experiments on Air Quality over Pearl River Delta of China, 2008b.

Liu, Z., Wang, Y., Vrekoussis, M., Richter, A., Wittrock, F., Burrows, J. P., Shao, M., Chang, C.-C., Liu, S.-C., Wang, H., and Chen, C.: Exploring the missing source of glyoxal (CHOCHO) over China, Geophysical Research Letters, 39, n/a–n/a, doi:10.1029/2012GL051645, http://dx.doi.org/10.1029/2012GL051645, 2012.

Maarten van het Bolscher, Tinus Pulles, R. B.: REanalysis of the TROpospheric chemical composition over the past 40 years A long-term global modeling study of tropospheric chemistry funded under the 5th EU framework programme EU-Contract No. EVK2-CT-2002-00170, Tech. rep., TNO, 2007.

Mao, J., Paulot, F., Jacob, D. J., Cohen, R. C., Crounse, J. D., Wennberg, P. O., Keller, C. A., Hudman, R. C., Barkley, M. P., and Horowitz, L. W.: Ozone and organic nitrates over the eastern United States: Sensitivity to isoprene chemistry, Journal of Geophysical Research: Atmospheres, 118, 11,256–11,268, doi:10.1002/jgrd.50817, http://dx.doi.org/10.1002/jgrd.50817, 2013.

Martin, R. V., Jacob, D. J., Yantosca, R. M., Chin, M., and Ginoux, P.: Global and regional decreases in tropospheric oxidants from photochemical effects of aerosols, Journal of Geophysical Research: Atmospheres, 108, n/a–n/a, doi:10.1029/2002JD002622, http://dx.doi.org/10.1029/2002JD002622, 4097, 2003.

Neu, J. L., Prather, M. J., and Penner, J. E.: Global atmospheric chemistry: Integrating over fractional cloud cover, Journal of Geophysical Research: Atmospheres, 112, n/a–n/a, doi:10.1029/2006JD008007, http://dx.doi.org/10.1029/2006JD008007, 2007.

Nishino, N., Arey, J., and Atkinson, R.: Formation Yields of Glyoxal and Methylglyoxal from the Gas-Phase OH Radical-Initiated Reactions of Toluene, Xylenes, and Trimethylbenzenes as a Function of NO2 Concentration, The Journal of Physical Chemistry A, 114, 10 140–10 147, doi:10.1021/jp105112h, http://pubs.acs.org/doi/abs/10.1021/jp105112h, 2010.

Palmer, P. I., Abbot, D. S., Fu, T.-M., Jacob, D. J., Chance, K., Kurosu, T. P., Guenther, A., Wiedinmyer, C., Stanton, J. C., Pilling, M. J., Pressley, S. N., Lamb, B., and Sumner, A. L.: Quantifying the seasonal and interannual variability of North American isoprene emissions using satellite observations of the formaldehyde column, Journal of Geophysical Research: Atmospheres, 111, n/a–n/a, http://dx.doi.org/10.1029/2005JD006689, 2006.

Shao, M., Zhang, Y., Zeng, L., Tang, X., Zhang, J., Zhong, L., and Wang, B.: Ground-level ozone in the Pearl River Delta and the roles of {VOC} and {NOx} in its production, Journal of Environmental Management, 90, 512 – 518, doi:http://dx.doi.org/10.1016/j.jenvman.2007.12.008, http://www.sciencedirect.com/science/article/pii/S0301479707004185, 2009.

Spurr, R. J. D.: LIDORT V2PLUS: a comprehensive radiative transfer package for UV/VIS/NIR nadir remote sensing, Proc. SPIE, 5235, 89–100, doi:10.1117/12.511103, 2004.

Stavrakou, T., Müller, J.-F., De Smedt, I., Van Roozendael, M., Kanakidou, M., Vrekoussis, M., Wittrock, F., Richter, A., and Burrows, J. P.: The continental source of glyoxal estimated by the synergistic use of spaceborne measurements and inverse modelling, Atmospheric Chemistry and Physics, 9, 8431–8446, doi:10.5194/acp-9-8431-2009, http://www.atmos-chem-phys.net/9/8431/2009/, 2009.

Valin, L. C., Russell, A. R., and Cohen, R. C.: Variations of OH radical in an urban plume inferred from NO2 column measurements, Geophysical Research Letters, 40, 1856–1860, doi:10.1002/grl.50267, http://dx.doi.org/10.1002/grl.50267, 2013.

van Donkelaar, A., Martin, R. V., Leaitch, W. R., Macdonald, A. M., Walker, T. W., Streets, D. G., Zhang, Q., Dunlea, E. J., Jimenez, J. L., Dibb, J. E., Huey, L. G., Weber, R., and Andreae, M. O.: Analysis of aircraft and satellite measurements from the Intercontinental Chemical Transport Experiment (INTEX-B) to quantify long-range transport of East Asian sulfur to Canada, Atmospheric Chemistry and Physics, 8, 2999–3014, doi:10.5194/acp-8-2999-2008, http://www.atmos-chem-phys.net/8/2999/2008/, 2008.

Volkamer, R., Platt, U., and Wirtz, K.: Primary and Secondary Glyoxal Formation from Aromatics: Experimental Evidence for the Bicycloalkyl-Radical Pathway from Benzene, Toluene, and p-Xylene, The Journal of Physical Chemistry A, 105, 7865–7874, doi:10.1021/jp010152w, http://dx.doi.org/10.1021/jp010152w, 2001.

Volkamer, R., Spietz, P., Burrows, J., and Platt, U.: High-resolution absorption cross-section of glyoxal in the UV–vis and {IR} spectral ranges, Journal of Photochemistry and Photobiology A: Chemistry, 172, 35 – 46, 2005.

Vrekoussis, M., Wittrock, F., Richter, A., and Burrows, J. P.: GOME-2 observations of oxygenated VOCs: what can we learn from the ratio glyoxal to formaldehyde on a global scale?, Atmospheric Chemistry and Physics, 10, 10 145–10 160, doi:10.5194/acp-10-10145-2010, http://www.atmos-chem-phys.net/10/10145/2010/, 2010.

Wang, X., Zhang, Y., Hu, Y., Zhou, W., Lu, K., Zhong, L., Zeng, L., Shao, M., Hu, M., and Russell, A. G.: Process analysis and sensitivity study of regional ozone formation over the Pearl River Delta, China, during the PRIDE-PRD2004 campaign using the Community Multiscale Air Quality modeling system, Atmospheric Chemistry and Physics, 10, 4423–4437, doi:10.5194/acp-10-4423-2010, http://www.atmos-chem-phys.net/10/4423/2010/, 2010.

Wild, O., Zhu, X., and Prather, M.: Fast-J: Accurate Simulation of In- and Below-Cloud Photolysis in Tropospheric Chemical Models, Journal of Atmospheric Chemistry, 37, 245–282, doi:10.1023/A:1006415919030, http://dx.doi.org/10.1023/A%3A1006415919030, 2000.

Xue, L. K., Wang, T., Gao, J., Ding, A. J., Zhou, X. H., Blake, D. R., Wang, X. F., Saunders, S. M., Fan, S. J., Zuo, H. C., Zhang, Q. Z., and Wang, W. X.: Ground-level ozone in four Chinese cities: precursors, regional transport and heterogeneous processes, Atmospheric Chemistry and Physics, 14, 13 175–13 188, 2014.

Zhang, J., Wang, T., Chameides, W. L., Cardelino, C., Kwok, J., Blake, D. R., Ding, A., and So, K. L.: Ozone production and hydrocarbon reactivity in Hong Kong, Southern China, Atmospheric Chemistry and Physics, 7, 557–573, doi:10.5194/acp-7-557-2007, http://www.atmos-chem-phys.net/7/557/2007/, 2007.

Zhang, Q., Streets, D. G., Carmichael, G. R., He, K. B., Huo, H., Kannari, A., Klimont, Z., Park, I. S., Reddy, S., Fu, J. S., Chen, D., Duan, L., Lei, Y., Wang, L. T., and Yao, Z. L.: Asian emissions in 2006 for the NASA INTEX-B mission, Atmospheric Chemistry and Physics, 9, 5131–5153, doi:10.5194/acp-9-5131-2009, http://www.atmos-chem-phys.net/9/5131/2009/, 2009.

Zhang, Y., Su, H., Zhong, L., Cheng, Y., Zeng, L., Wang, X., Xiang, Y., Wang, J., Gao, D., Shao, M., Fan, S., and Liu, S.: Regional ozone pollution and observation-based approach for analyzing ozone–precursor relationship during the PRIDE-PRD2004 campaign, Atmospheric Environment, 42, 6203 – 6218, doi:http://dx.doi.org/10.1016/j.atmosenv.2008.05.002, http://www.sciencedirect.com/science/article/pii/S1352231008003701, pRIDE-PRD 2004 Campaign : Program of Regional Integrated Experiments on Air Quality over Pearl River Delta of China, 2008.

Zheng, J., Shao, M., Che, W., Zhang, L., Zhong, L., Zhang, Y., and Streets, D.: Speciated VOC Emission Inventory and Spatial Patterns of Ozone Formation Potential in the Pearl River Delta, China, Environmental Science and Technology, 43, 8580–8586, doi:10.1021/es901688e, http://dx.doi.org/10.1021/es901688e, pMID: 20028055, 2009a.

Zheng, J., Zhang, L., Che, W., Zheng, Z., and Yin, S.: A highly resolved temporal and spatial air pollutant emission inventory for the Pearl River Delta region, China and its uncertainty assessment, Atmospheric Environment, 43, 5112 – 5122, doi:http://dx.doi.org/10.1016/j.atmosenv.2009.04.060, http://www.sciencedirect.com/science/article/pii/S1352231009004130, 2009b.

Zheng, J., Zheng, Z., Wang, Z., Zhong, L., and Wu, D.: Biogenic VOCs emission inventory and its temporal and spatial characteristics in the Pearl River Delta area (in Chinese), China Environ. Sci., 29, 345–350, 2009c.

Zheng, J., Zheng, Z., Yu, Y., and Zhong, L.: Temporal, spatial characteristics and uncertainty of biogenic {VOC} emissions in the Pearl River Delta region, China, Atmospheric Environment, 44, 1960 – 1969, doi:http://dx.doi.org/10.1016/j.atmosenv.2010.03.001, http://www.sciencedirect.com/science/article/pii/S1352231010001858, 2010.

Zhong, L., Louie, P. K., Zheng, J., Yuan, Z., Yue, D., Ho, J. W., and Lau, A. K.: Science–policy interplay: Air quality management in the Pearl River Delta region and Hong Kong, Atmospheric Environment, 76, 3 – 10, 2013.

Zhu, L., Jacob, D. J., Mickley, L. J., Marais, E. A., Cohan, D. S., Yoshida, Y., Duncan, B. N., Abad, G. G., and Chance, K. V.: Anthropogenic emissions of highly reactive volatile organic compounds in eastern Texas inferred from oversampling of satellite (OMI) measurements of HCHO columns, Environmental Research Letters, 9, 114 004, http://stacks.iop.org/1748-9326/9/i=11/a=114004, 2014.

Zhu, L., Jacob, D. J., Kim, P. S., Fisher, J. A., Yu, K., Travis, K. R., Mickley, L. J., Yantosca, R. M., Sulprizio, M. P., De Smedt, I., Gonzalez Abad, G., Chance, K., Li, C., Ferrare, R., Fried, A., Hair, J. W., Hanisco, T. F., Richter, D., Scarino, A. J., Walega, J., Weibring, P., and Wolfe, G. M.: Observing atmospheric formaldehyde (HCHO) from space: validation and intercomparison of six retrievals from four satellites (OMI, GOME2A, GOME2B, OMPS) with SEAC 4 RS aircraft observations over the Southeast US, Atmospheric Chemistry and Physics Discussions, 2016, 1–24, doi:10.5194/acp-2016-162, http://www.atmos-chem-phys-discuss.net/acp-2016-162/, 2016.

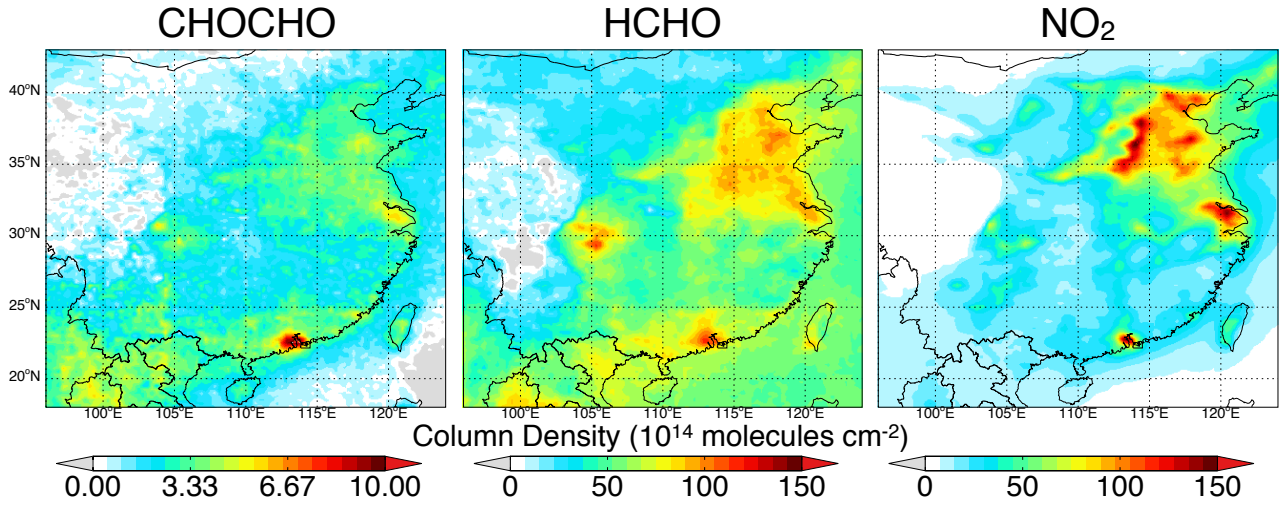

Figure 1. Annual mean vertical column densities of NO_2, HCHO, and CHOCHO for 2006-2007. Values are OMI observations from Chan Miller et al. (2014) for CHOCHO, González Abad et al. (2015) for HCHO, and Bucsela et al. (2013). for NO_2

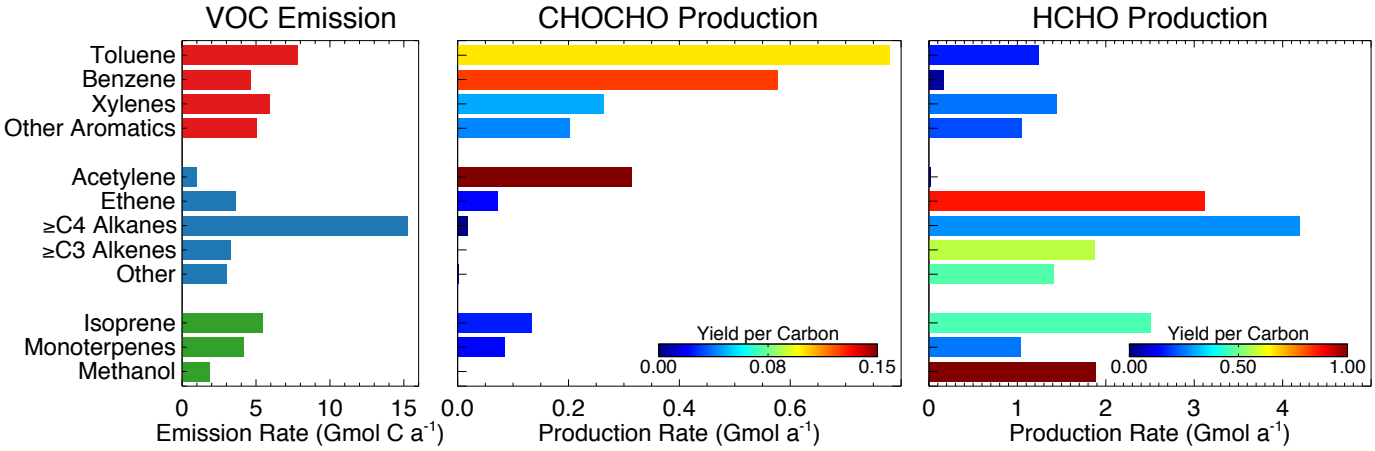

Figure 2. Yearly VOC emissions (2006) in the PRD ($21.5-24°$N, $112-115.5°$E) and corresponding yields and production rates of CHOCHO and HCHO over one day of aging. VOC emissions are from Zheng et al. (2009a). Yields are computed using the MCMv3.2 chemical mechanism(Jenkin et al., 1997, 2003).

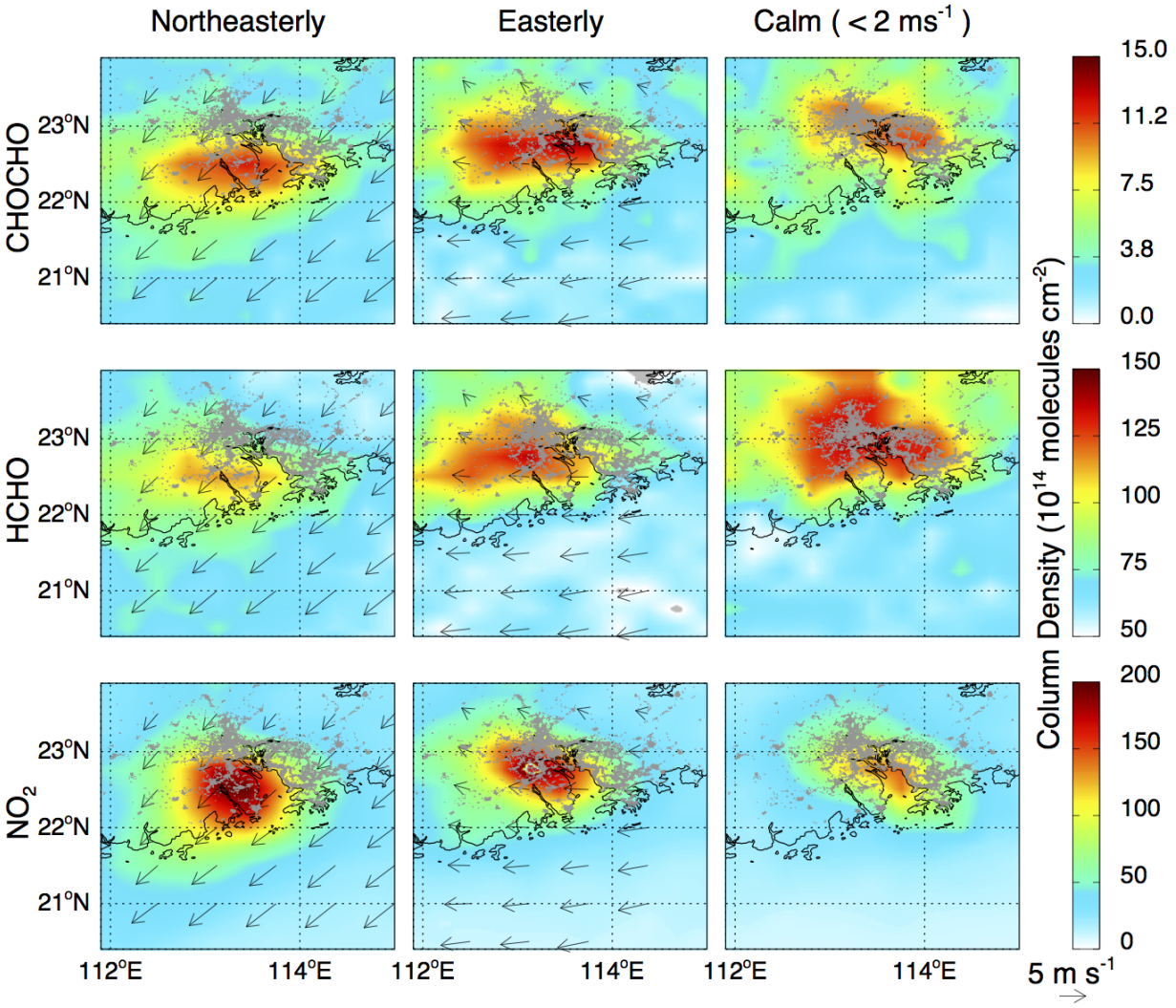

Figure 3. Mean OMI vertical column densities of CHOCHO, HCHO, and NO_2 over the PRD for 2006 to 2007, segregated by wind direction. Winds vectors at 60-m altitude are from the NASA GEOS-5 assimilated meteorology product. The distribution of urban landcover from the MODIS type 5 land cover product is shown in grey.

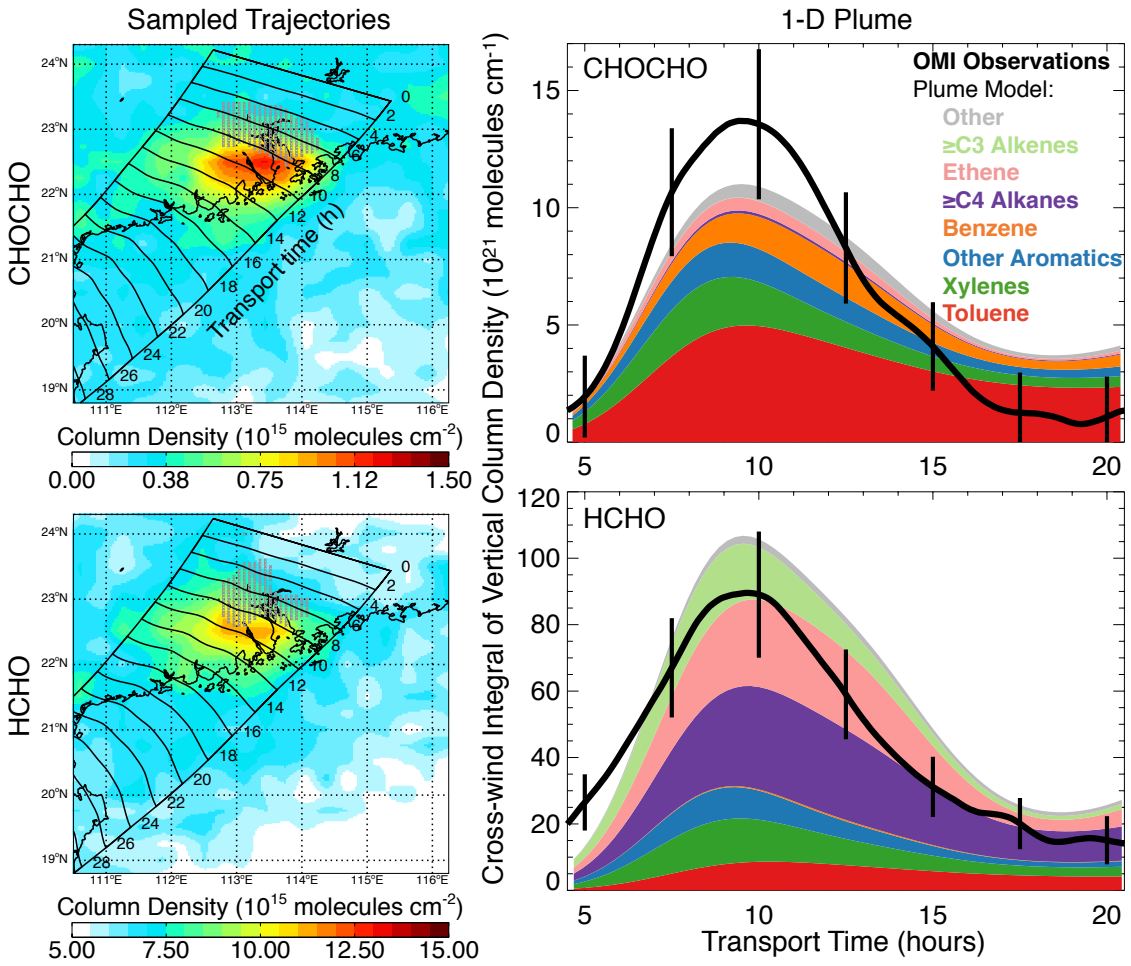

Figure 4. Mean CHOCHO and HCHO PRD plumes under northeasterly flow conditions. **Left:** Vertical column densities, overlaid with surface air (60 m) trajectories for the mean wind field of Figure 3. The trajectories are initialized upwind of the PRD ($t = 0$), and transport times in hours along the trajectories are indicated. The grey hatched area indicates the location of maximum emissions as diagnosed by the peak concentrations for the calm wind conditions in Figure 3 (8×10^{14} and 1.25×10^{16} molecules cm^{-2} for CHOCHO and HCHO respectively). **Right:** CHOCHO and HCHO cross-wind integrals of vertical column density. The OMI observations are line integrals across the trajectories in the left panels, and vertical bars are retrieval uncertainties. The stacked contours are results from the 1-D plume model showing the contributions from individual VOCs as given by the Zheng et al. (2009a) PRD inventory, combined with the CHOCHO and HCHO yields of Figure 2. VOC emissions in the plume model for CHOCHO and HCHO are centered at transport time $t = 6.5$ and $t = 7.0$ hours respectively, based on the plume location during calm wind conditions.

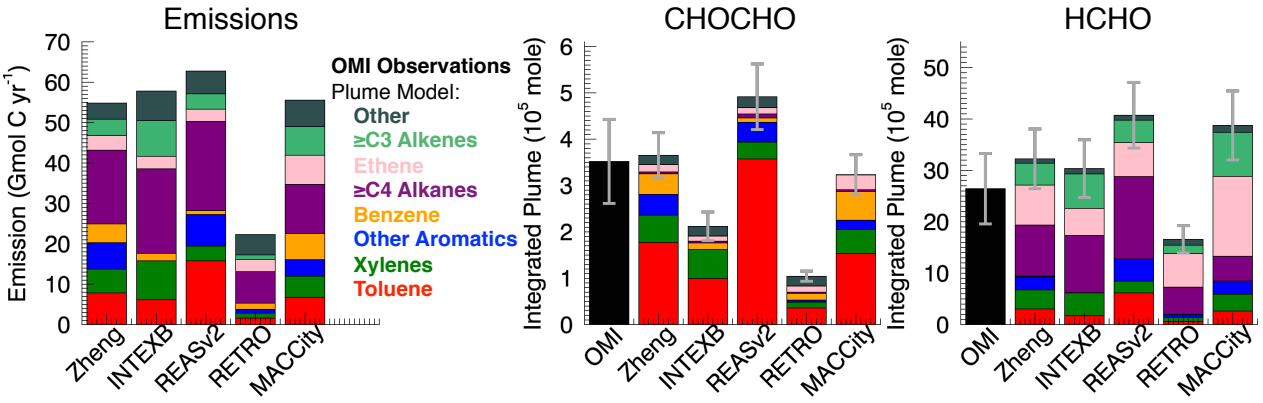

Figure 5. VOC emissions in the PRD from five different inventories (see text), and corresponding plume amounts of CHOCHO and HCHO as computed from the plume model discussed in the text and integrated from $t = 5$ to $t = 20$ h on the trajectory time grid shown in Figure 4. Model uncertainty bars are from uncertainties in OH concentrations and photolysis rates (see text). OMI observations integrated on the same trajectory grid are also shown.

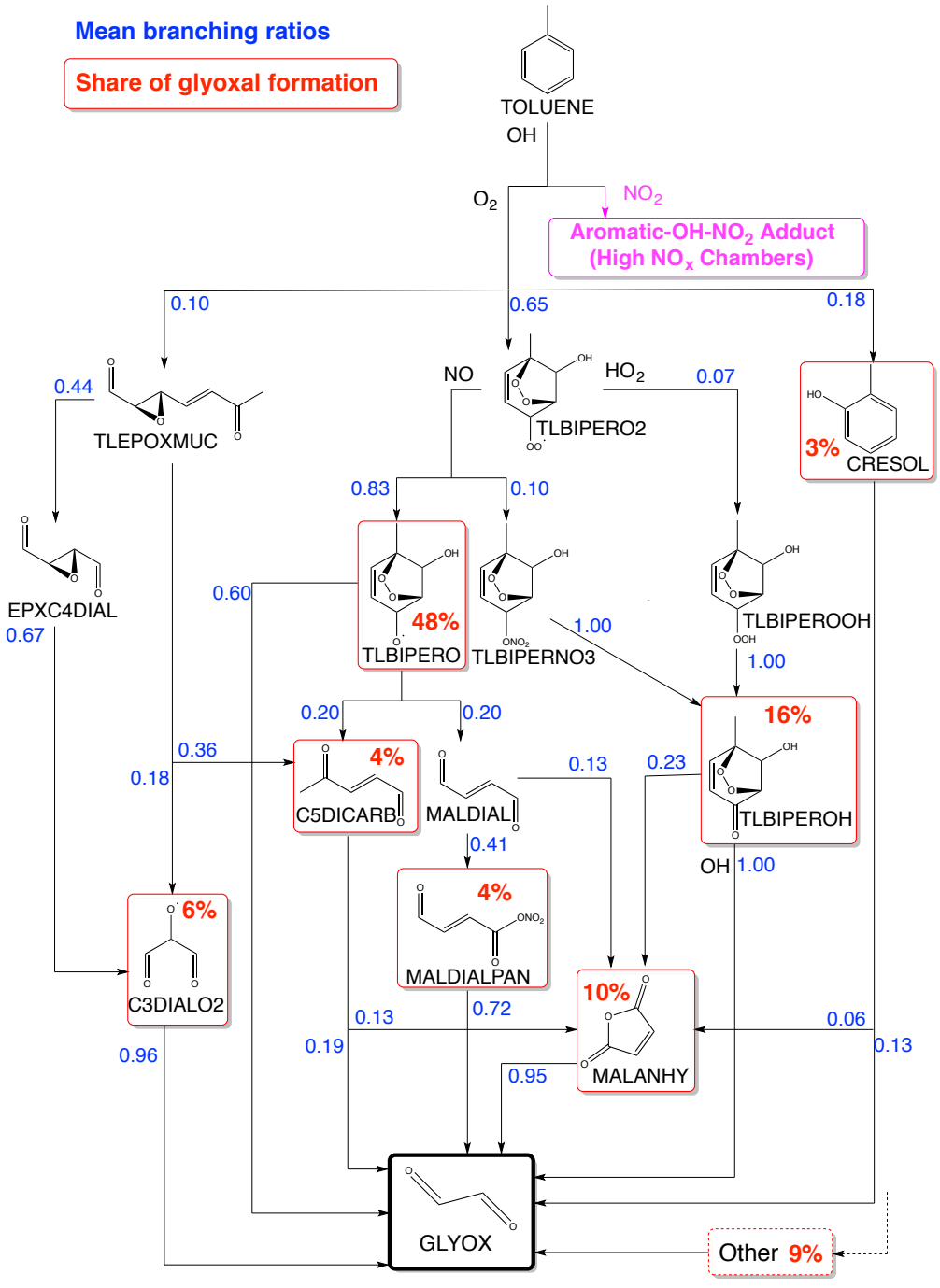

Figure 6. Pathways to glyoxal formation from toluene oxidation by OH in MCMv3.2. Only species relevant to CHOCHO formation are shown, and are labeled by their MCMv3.2 name. Branching ratios (blue) and the share of glyoxal formation from each boxed species (red) are from the 24 h box model simulation described in the text. The high NO_2 pathway (not in MCMv3.2 but relevant in chamber studies) is indicated in pink.